https://doi.org/10.5194/bg-2021-261
Preprint. Discussion started: 21 October 2021

Biogeosciences Discussions
Open Access

Strong influence of trees outside forest in regulating microclimate of intensively modified Afromontane landscapes

Iris J. Aalto[1], Eduardo E. Maeda[1], Janne Heiskanen[1,2], Eljas K. Aalto[3], Petri K. E. Pellikka[1]

[1]Department of Geosciences and Geography, University of Helsinki, P.O. Box 64, FI-00014, Helsinki, Finland
[2]Institute for Atmospheric and Earth System Research, Faculty of Science, University of Helsinki, Finland
[3]Department of Economics, Turku School of Economics, 20014 University of Turku, Finland

Correspondence to: Iris Aalto (iris.aalto@helsinki.fi)

Abstract. Climate change is expected to have detrimental consequences on fragile ecosystems, threatening biodiversity as well as food security of millions of people. Trees are likely to play a central role in mitigating these impacts. The microclimatic conditions below tree canopies usually differ substantially from the ambient macroclimate, as vegetation can buffer temperature changes and variability. Trees cool down their surroundings through several biophysical mechanisms, and the cooling benefits occur also with trees outside forest. The aim of this study was to examine the effect of canopy cover on microclimate in an intensively modified Afromontane landscape in Taita Taveta, Kenya. We studied temperatures recorded by 19 microclimate sensors under different canopy covers, and land surface temperature (LST) estimated by Landsat 8 thermal infrared sensor. We combined the temperature records with high–resolution airborne laser scanning data to untangle the combined effects of topography and canopy cover on microclimate. We developed four multivariate regression models to study the joint impacts of topography and canopy cover on LST. The results showed a negative linear relationship between canopy cover percentage and daytime mean (R^2 = 0.65) and maximum (R^2 = 0.75) temperatures. Any increase in canopy cover contributed to reducing temperatures. The average difference between 0% and 100% canopy cover sites was 5.7 ˚C in mean temperatures and 10.2 ˚C in maximum temperatures. Canopy cover reduced LST on average by 0.05 ˚C/%CC. The influence of canopy cover on microclimate was shown to vary strongly with elevation and ambient temperatures. These results demonstrate that trees have substantial effect on microclimate, but the effect is dependent on macroclimatic conditions, highlighting the importance of maintaining tree cover particularly in warmer conditions. Hence, we demonstrate that trees outside forests can increase climate change resilience in fragmented landscapes, having strong potential for regulating regional and local temperatures.

Keywords

Agroforestry, airborne laser scanning, canopy cover, land surface temperature, Landsat 8, microclimate

https://doi.org/10.5194/bg-2021-261
Preprint. Discussion started: 21 October 2021

1. Introduction

Climate change poses an imminent threat to the rich biodiversity and frequently found fragile socio–economic conditions that characterize Afromontane ecosystems and their surroundings. In these regions, climate warming is mostly driven by land use and land cover change (LULCC) (IPCC, 2018; Pellikka and Hakala, 2019; Abera et al., 2020). Agricultural expansion, in particular, has caused rapid loss of tropical forests (FAO, 2016). Forests are essential in mitigating climate warming, due to their role in especially the carbon and water cycles (Beer et al. 2010; Ellison et al. 2017; De Frenne et al. 2019).

Currently, forests cover approximately 4 billion hectares of the Earth's surface (FAO, 2016). Trees that are not part of a forest are commonly called "trees outside forest" (TOF) and, by the definition of FAO (2000), include trees on farmland, in cities, and in other locations not defined as forest. Forests and TOF provide vital ecosystem services including water regulation, air purification, carbon sequestration, and climate regulation. They are also a source of goods for humans (Martínez Pastur et al., 2018). Many ecosystem services, such as nutrient cycling and pollination, occur in the understories, where tree canopies create the appropriate microclimates essential for these processes (De Frenne et al., 2013). The term "microclimate" describes the climatic conditions near the ground or along the vertical forest profile, with a scale from centimeters to meters (Zellweger et al., 2019). In contrast to free air temperatures, which are highly controlled by elevation and atmospheric processes, temperatures close to the ground are primarily affected by topographic factors and vegetation structures that produce local microclimates through shading, mixing of air, and evapotranspiration (Das et al., 2015; Zellweger et al., 2020). Climatic conditions below forest canopies can differ substantially from the ambient macroclimate. Furthermore, they can vary spatially within the forest (Chen et al., 1999). This variability has different magnitudes at different latitudes: for example, tropical forests experience the strongest cooling effect (Li et al., 2015; Wanderley et al., 2019). The temperature buffering provided by tree cover may protect ecosystems from climate change consequences (Zomer et al., 2016; Ellison et al., 2017; De Frenne et al., 2019; Wanderley et al., 2019), but the magnitude of the buffering is affected by the forest area (Ewers and Banks-Leite, 2013). In time, forest microclimates will likely warm like the macroclimate around them, and fragmentation may accelerate this process (Ewers and Banks-Leite, 2013; Li et al., 2016).

Studies about forests' response to climate warming have primarily focused on the macroscale, despite wide recognition of the vital role microclimates play (Belsky et al., 1989; De Frenne et al., 2019). Further, microclimate may be a better indicator of how well forests mitigate climate change than macroclimate (De Frenne et al., 2013). Due to the importance of microclimatic conditions for the survival of tropical species facing climate change, below–canopy microclimates warrant further investigation (Jucker et al., 2018).

https://doi.org/10.5194/bg-2021-261
Preprint. Discussion started: 21 October 2021

However, microclimatic studies require extensive field measurements, making them sometimes unpractical or imprecise in larger scale applications (Prata et al., 1995). Alternatively, measuring satellite–derived land surface temperature (LST) proves useful when point-wise field measurements are insufficient, given the high spatial coverage of spaceborne LST and the strong correlation between LST and air temperature (Jin and Dickinson, 2010; Li et al., 2013). However, LST cannot provide information in the smallest relevant scales, such as organism level (Potter et al., 2013; Jucker et al., 2018). Due to the various factors affecting LST, accurate estimation remains a challenge (Simó et al., 2018; Li et al., 2013). Nevertheless, the complexity of the issue with climate change requires attention at both spatial resolutions.

In remote sensing of vegetation, common outputs in previous research are land cover and land use types or vegetation indices, such as the normalized vegetation index (NDVI) or leaf area index (LAI) (Nemani et al., 1993; Kim 2013; He et al., 2019). However, airborne laser scanning (ALS) has proven to be a more effective method for computing structural variables, such as above-ground biomass, canopy height, and canopy cover (Griffin et al., 2008; Heiskanen et al., 2015a; Heiskanen et al., 2015b; Pellikka et al., 2018; Jucker et al., 2018). Canopy cover (CC) describes the proportion of the forest floor covered by the vertical projection of the tree crowns (Korhonen et al., 2006) and it is the most important variable used in defining forests or other land with tree cover (FAO, 2015). ALS can assess tree cover over large areas more precisely than field measurements can. Hence, when ALS is combined with either field-based or remotely sensed temperatures, we can study the influence of trees on temperature in a new way of that is both nuanced and large scale.

The primary objective of this study was to examine how different levels of CC can contribute to lower temperatures and more stable microclimates across a highly heterogeneous Afromontane landscape in Kenya. We based our analysis on micro-climatological measurements and CC estimates retrieved from ALS data. Microclimate sensors cannot entirely capture the spatial variability of temperatures, especially in heterogeneous landscapes. Therefore, we used satellite thermal data to provide a comprehensive and spatially continuous representation of the relationship between CC and temperature.

2. Materials and methods

2.1 Study area

The Taita Hills are located in the Taita-Taveta County in the Coast Province in southern Kenya, approximately 200 km from Mombasa and 360 km from the capital city Nairobi. The study area comprises of the Taita Hills and the lowland areas of Maktau, LUMO Community Wildlife Sanctuary and Taita Hills Wildlife Sanctuary that have been laser scanned by University of Helsinki (Fig. 1). The elevation in the study area varies from 640 m in the lowlands to the highest peak of the hills, Vuria, at 2208 m. Climate is mainly semi-arid. According to the Kenya Ministry of Agriculture, Livestock and Fishery (MoALF), annual precipitation averages 650 mm, but differences between hills and lowlands are notable: lowlands receive 500 mm annually compared to 1500 mm in the hills. Two rainy seasons control the climate and growing seasons: long rains from March to June, and short rains from October to December (Pellikka et al., 2013), while months from January to March are a short hot dry season and months from June to October long cool dry season (Wachiye et al., 2020). Mean temperature in the lowlands is 23 °C and in the hills 18 °C (MoALF, 2016). Vegetation varies from dry savanna and shrubland in the lowlands dominated by *Vachellia ssp.* and *Commiphora ssp*. tree species to indigenous cloud forests in the hilltops. Small indigenous forest fragments, exotic tree plantations, and intensive agriculture dominate the landscape in the hills. Agroforestry practices are typical, which increases cropland CC. TOF make up a remarkable amount of the area's total aboveground carbon and play an important part in carbon sequestration in the area (Pellikka et al., 2018), especially because Taita Hills have experienced massive indigenous forest loss since 1950's (Pellikka et al., 2009). Forest loss is a major threat to biodiversity, as Taita Hills are identified as an important biodiversity hotspot (Pellikka et al., 2013; Thijs et al., 2015).

With climate change, temperatures in Kenya are expected to increase by 2–4 °C by the end of the century (Adhikari et al., 2015), and changes in precipitation, that will increase the moisture stress of crops, are projected (MoALF, 2016). Dry spells, heat stress and extreme rain events pose a threat to the area's agricultural production. These phenomena cause crop failure and low yields, and hence affect the livelihoods of people (Adhikari et al., 2015; MoALF 2016). Farmers in the area have already noticed climate fluctuations that affect both crops and livestock (Mwalusepo et al., 2015).

https://doi.org/10.5194/bg-2021-261
Preprint. Discussion started: 21 October 2021

Biogeosciences
Discussions
Open Access

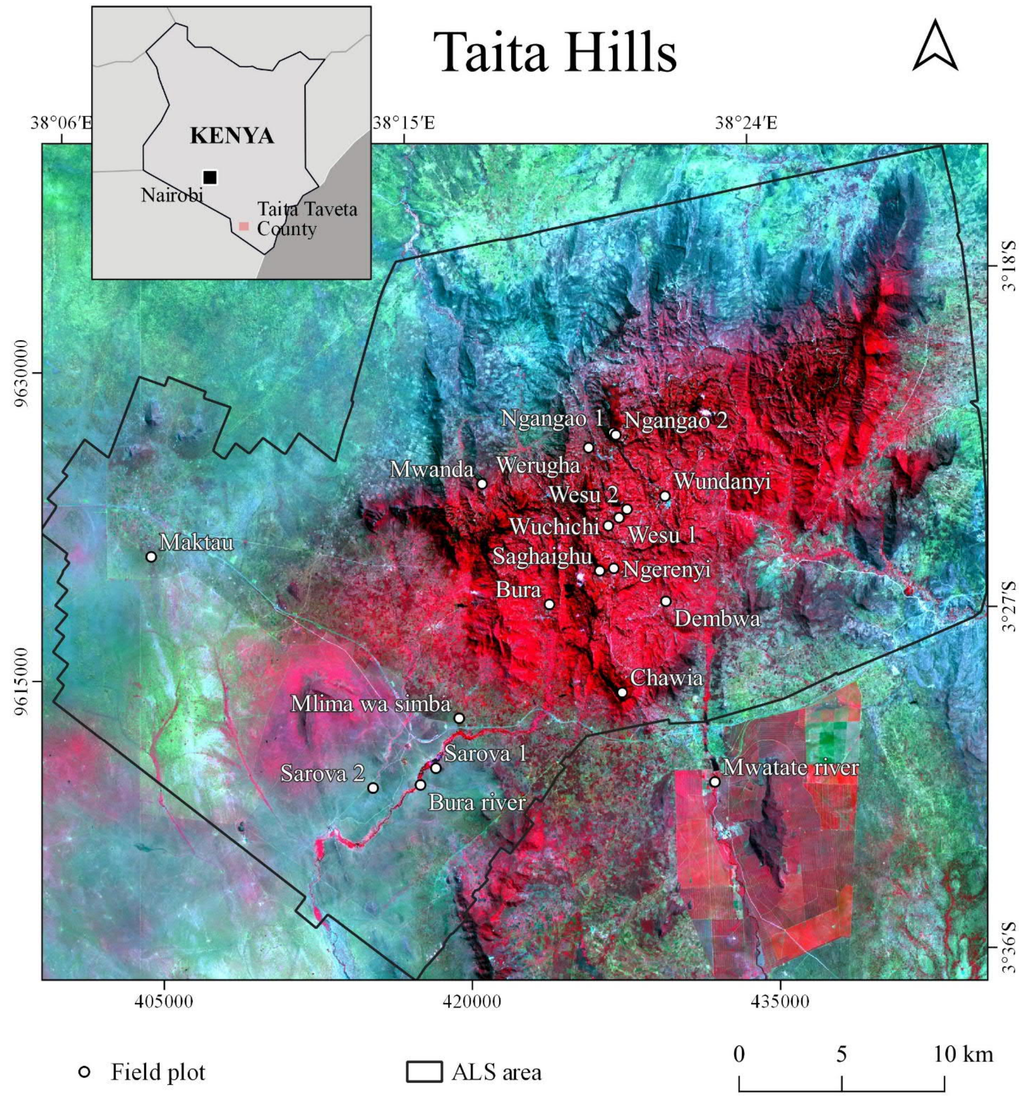

108

109 **Figure 1:** Field plots with microclimate sensors in Taita Taveta County, Kenya. The base map is a false color Landsat 8

110 OLI image from July 4, 2019.

111

112 **2.2 Airborne laser scanning data**

https://doi.org/10.5194/bg-2021-261
Preprint. Discussion started: 21 October 2021

We applied an ALS-based Digital Elevation Model (DEM) raster at 1 m resolution and a CC raster at 30 m resolution. The ALS data for the hills were acquired in February 2014 and February 2015, and the data for lowland areas in March 2014. The mean pulse density of the ALS data in the hills was 3.1 pulses/m^{-2} and mean return density 3.4 returns/m^{-2}, for the lowlands the pulse density was 1.04 pulses/m^{-2}. The ALS data used in this study are described in detail in Adhikari et al. (2017) and Amara et al. (2020) with the description of pre-processing and derivation of DEM and CC rasters.

We resampled the DEM to 30 m resolution to fit to the spatial resolution of the Landsat 8 image, and utilized it to derive topographic factors slope degree (°) and aspect (°) using ArcGIS Pro spatial analyst tools.

2.3 Microclimatological field measurements

Based on the CC raster derived from the ALS data, we selected a total of 19 field plots representing different CC levels (Table 1). In the plots, we installed TOMST TMS-4 microclimate sensors to measure temperature at three different heights: soil at 6 cm below ground, surface at 2 cm above ground, and air temperature at 15 cm above ground (T_{soil}, $T_{surface}$ and T_{air}, respectively) (Wild et al., 2019) from June 13 to July 10, 2019. The sensors measured parameters every 15 minutes. We calculated daytime temperature aggregates between sunrise and sunset, local time 06.30–18.30 UTC + 3h. We calculated maxima as the mean of daily maxima, and minimum temperatures as the mean of minimum temperatures based on the 24 hour cycle.

To isolate the influence of CC on microclimate, we quantified and later removed the effect of topography, such as elevation (m) and slope (°), on temperature. We examined the relationships between the variables first with Pearson's correlation using elevation, slope and CC as explanatory variables in a multiple regression model. Elevation and CC were the only statistically significant variables. We corrected the daytime mean temperatures according to the altitudinal lapse rates, which were 7.26 °C km^{-1} for soil temperature (T_{soil}), 8.09 °C km^{-1} for surface temperature ($T_{surface}$) and 8.06 °C km^{-1} for air temperature (T_{air}). In the case of diurnal analysis, we applied separate lapse rates for each hour. These varied from 6.1 °C to 8.2 °C km^{-1} in T_{soil}, 3.8 °C to 10.4 °C km^{-1} in $T_{surface}$ and 3.3 °C to °C km^{-1} in T_{air}. To find the relationships between temperature, CC and topographic variables, we conducted statistical analysis, including descriptive statistics, linear regression and Pearson's correlation. We used RStudio (R Core Team, 2019) for all statistical analysis.

Because the ALS data was 4–5 years older than the field measurements, we acquired hemispherical photography at each field plot for validating the CC raster. Moreover, the ALS data was collected during the short dry season, in contrast to the field measurements, which we carried out during the start of long dry season in June 2019. For Mwatate river plot, CC was retrieved by hemispherical photography only, as the plot was laying outside of the ALS coverage. The methodology is described in the supplementary material.

https://doi.org/10.5194/bg-2021-261
Preprint. Discussion started: 21 October 2021

Site	CC %	Elevation, m	Description
Bura	68	1095	Parkland by school campus
Bura river	79	880	Riverine forest
Chawia	97	1562	Indigenous forest
Dembwa	13	1083	Agroforestry
Maktau	19	1044	Bushland
Mlima wa simba	8	923	Bushland
Mwanda	2	1653	Bushland
Mwatate river	63	884	Riverine forest
Ngangao 1	94	1775	Indigenous forest
Ngangao 2	77	1778	Eucalyptus forest
Ngerenyi campus	44	1572	Macadamia plantation
Saghaighu	16	1611	Agroforestry
Sarova 1	0	901	Bushland
Sarova 2	0	900	Grassland
Werugha	8	1613	Macadamia plantation
Wesu 1	53	1642	Forest edge
Wesu 2	0	1562	Open maize field
Wuchichi	36	1595	Agroforestry
Wundanyi	31	1372	Riverside bushland

Table 1: Names, canopy cover (CC) percentages, elevations and descriptions of field plot sites.

2.4 Land Surface Temperature

To observe the effect of CC on temperature in Taita Taveta County, we applied Landsat 8 OLI thermal infrared sensor (TIRS) satellite image data, downloaded from USGS Earth Explorer (https://earthexplorer.usgs.gov/). The bands 10 and 11 of TIRS provide thermal infrared imagery in a resolution of 100 m, but we resampled the band to 30 m to concert with the OLI images. The image used in the study was a Level-1 scene obtained on July 4, 2019 at approximately 10:30 UTC + 3h with solar azimuth angle of 45.6° and solar elevation angle of 52.1°. The cloud cover of the whole scene was 11.67 %; there was no completely cloudless scene over the study area for the timing of the field measurements.

Several methods have been developed to retrieve LST from Landsat 8. Unfortunately, shortly after the launch of Landsat 8 in 2013, a stray light problem was detected with TIRS band 11, and it was not recommended by United States Geological

https://doi.org/10.5194/bg-2021-261
Preprint. Discussion started: 21 October 2021

Biogeosciences Discussions
Open Access
EGU

Survey (USGS) to apply for scientific purposes (USGS, 2017). In order to result in a topographically corrected LST product, we applied the workflow by Ndossi and Avdan (2016) (Fig. 2). We used the single channel (SC) method by Jiménez-Muñoz and Sobrino (2003) to calculate LST, because SC method needs only one thermal infrared channel, and land surface emissivity and water vapor content as parameters. The SC formula is shown in Eq. (1):

$$T_s = \gamma\left[\frac{1}{\varepsilon}(\Psi_1 L_{sen} + \Psi_2) + \Psi_3\right] + \delta \quad (1)$$

$$\gamma = \frac{T_{sen}^2}{b_\gamma L_{sen}} \quad (2)$$

$$\delta = T_{sen} - \frac{T_{sen}^2}{b_\gamma} \quad (3)$$

where Ts = LST, γ = parameter depending on Eq. (2), δ = parameter depending on Eq. (3), ε = land surface emissivity, L_{sen} = top of atmosphere spectral radiance (W sr^{-1} m^{-2} μm^{-1}), $b\gamma$ = 1324 K for Landsat 8 band 10, and T_{sen} = at sensor brightness temperature (K). We obtained the atmospheric parameters Ψ1, Ψ2 and Ψ3 with Eq. (4):

$$\begin{bmatrix}\Psi_1\\ \Psi_2\\ \Psi_3\end{bmatrix} = \begin{bmatrix}c_{11} & c_{12} & c_{13}\\ c_{21} & c_{22} & c_{23}\\ c_{31} & c_{32} & c_{33}\end{bmatrix}\begin{bmatrix}\omega^2\\ \omega\\ 1\end{bmatrix} \quad (4)$$

According to Jiménez-Muñoz, et al. (2014), the coefficients for atmospheric parameters for Landsat 8 TIRS are as in Eq. (5):

$$c = \begin{bmatrix}0.04019 & 0.02916 & 1.01523\\ -0.38333 & -1.50294 & 0.20324\\ 0.00918 & 1.36072 & -0.27514\end{bmatrix} \quad (5)$$

We conducted similar topographic correction with the Landsat image as with microclimate sensors to exclude the effect of topography on LST. Topographic variables (elevation, slope and aspect), CC and LST were included in a multiple regression model. We classified aspect to nine classes indicating eight cardinal directions (south, south-west, west, north-west, north, north-east, east, south-east), and flat surface. The classes were treated as dummy variables due to their categorical nature. Following Wanderley et al. (2019), we calculated the topographically corrected LST with Eq. (6):

$$T' = T - \Delta Th - \Delta Ts - \Delta Ta \quad (6)$$

Where T' = topographically corrected LST, T = raw LST, ΔTh = difference of T to the reference LST at elevation of 880 m, ΔTs = difference of T to the reference LST at slope of 0 °, ΔTa = difference of T to the reference LST in the aspect class "north". We used linear regression to study how much CC percentage and topographic variables affected microclimate and LST. In total, we estimated four different models for LST (Table 2).

https://doi.org/10.5194/bg-2021-261
Preprint. Discussion started: 21 October 2021

Model	Predictors
1	DEM, CC, slope, aspect (south, south-west, west, north-west, north, north-east, east, south-east)
2	DEM, CC, slope, aspect (south, south-west, west, north-west, north, north-east, east, south-east) elevation zones (<1000 m, 1000–1500 m, >1500 m), elevation zones * CC
3	DEM, CC, slope, aspect (south, south-west, west, north-west, north, north-east, east, south-east), DEM * CC
4	DEM, CC, slope, aspect (south, south-west, west, north-west, north, north-east, east, south-east), elevation zones (<1000 m, 1000–1500 m, >1500 m), elevation zones * CC, aspect classes * CC

Table 2: Topographic and canopy cover (CC) predictors included in the four multiple regression models used in the analysis of Landsat 8 Land surface temperature.

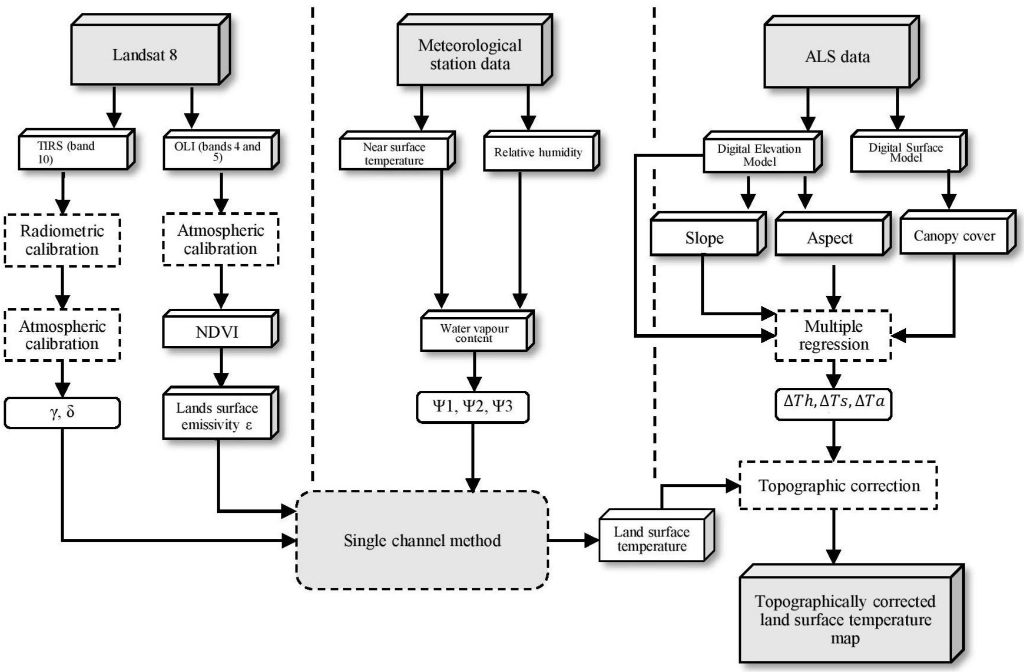

Figure 2: The workflow of Landsat 8 processing following the methodology by Ndossi and Avdan (2016), and topographic correction.

https://doi.org/10.5194/bg-2021-261
Preprint. Discussion started: 21 October 2021

3. Results

3.1 Canopy cover and microclimate

3.1.1 Temporal variation

Figure 3 presents the daily variation in topographically corrected daytime mean temperatures (T'). The effect of CC was evident at all three measurement heights (soil, surface, air): mean temperatures were lower in high CC sites than in open areas, yet some low CC sites exhibited relatively low temperatures. On the hottest day of the study period (July 2), temperature differences between the hottest (Maktau, 19% CC) and coolest (Ngangao 1, 94% CC) sites were 11.0 °C in T'_{soil}, 11.3 °C in $T'_{surface}$ and 9.8 °C in T'_{air}. Even during colder days, temperatures were approximately 6.5 °C lower in sites with dense canopies than in open land.

CC affected also temperature variability: SD of temperature decreased by approximately 0.1 per 10 CC% increase at all measurement heights. Especially T'_{soil} in the sites with high CC remained relatively stable from day to day, showing little fluctuation even during the hot day streaks: differences remained even less than 1 °C between hottest and coolest days.

When comparing the three measurement heights, the coldest mean temperatures were measured in T'_{air} and the hottest in $T'_{surface}$. Temperatures varied more in $T'_{surface}$ (SD = 3.0) and T'_{air} (SD = 2.7) than in T'_{soil} (SD = 2.3).

https://doi.org/10.5194/bg-2021-261
Preprint. Discussion started: 21 October 2021

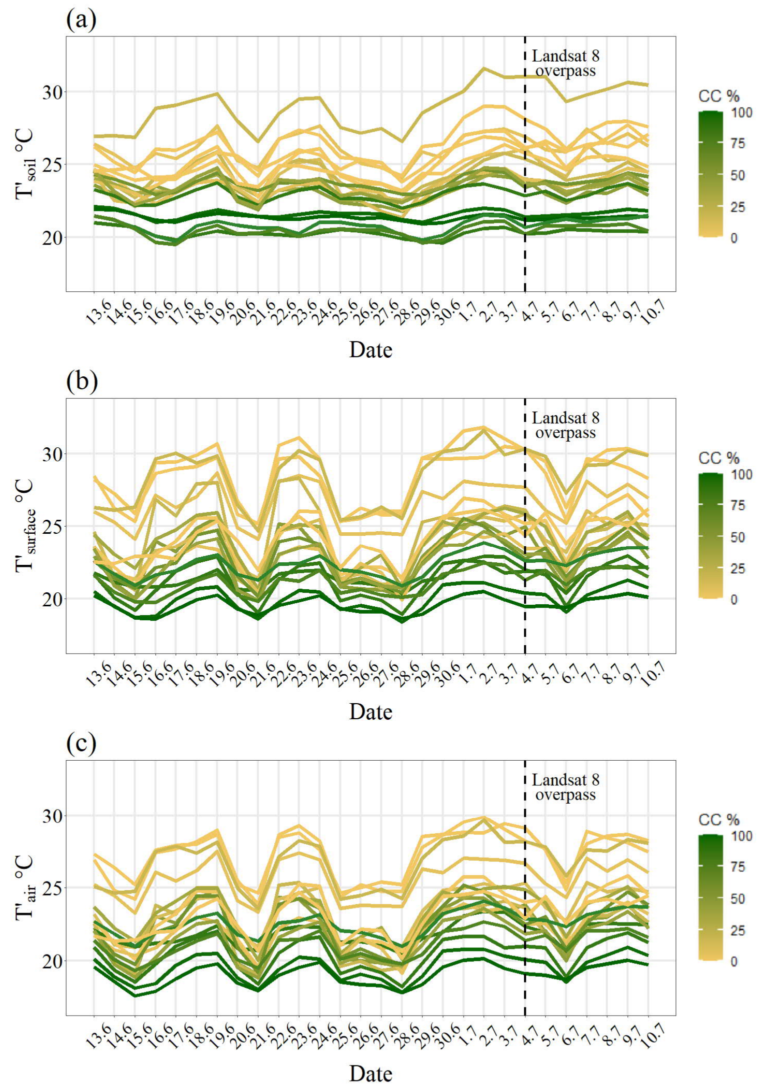

Figure 3: Daily variation in topographically corrected daytime (6.30–18.30) mean temperatures (T') between June 13 and July 10, 2019. Line color indicates canopy cover (CC) percentage. Dashed line represents the overpass date of Landsat 8, July 4, 2019. a) Soil temperature. b) Surface temperature. c) Air temperature.

Figure 4 shows the intra-daily temperature variability based on study period means. T'_{soil} were more stable than $T'_{surface}$ and T'_{air} that showed higher peaks and drops. In the morning, temperatures at all measurement heights started to rise rapidly between 6:00 and 8:00. Changes in T'_{soil} seemed to lag a couple of hours behind $T'_{surface}$ and T'_{air}: they reached highest readings between 11:00 and 15:00, while T'_{soil} peaked between 15:00 and 17:00. Further, after peaking,

https://doi.org/10.5194/bg-2021-261
Preprint. Discussion started: 21 October 2021

temperatures decreased before stabilizing between 19:00 and 20:00 in $T'_{surface}$ and T'_{air}, while T'_{soil} decreased slower. T_{soil} remained warmer during the night than the other two.

Figure 4 also describes the correlation between CC% and temperatures. The impact of CC was the lowest in the morning, when the temperatures also reached their minima. The strongest correlation (r < -0.8) occurred during afternoon at all measurement heights. T'_{soil} correlated negatively with CC% throughout the day, in contrast to $T'_{surface}$ and T'_{air}, where correlations were positive during the night.

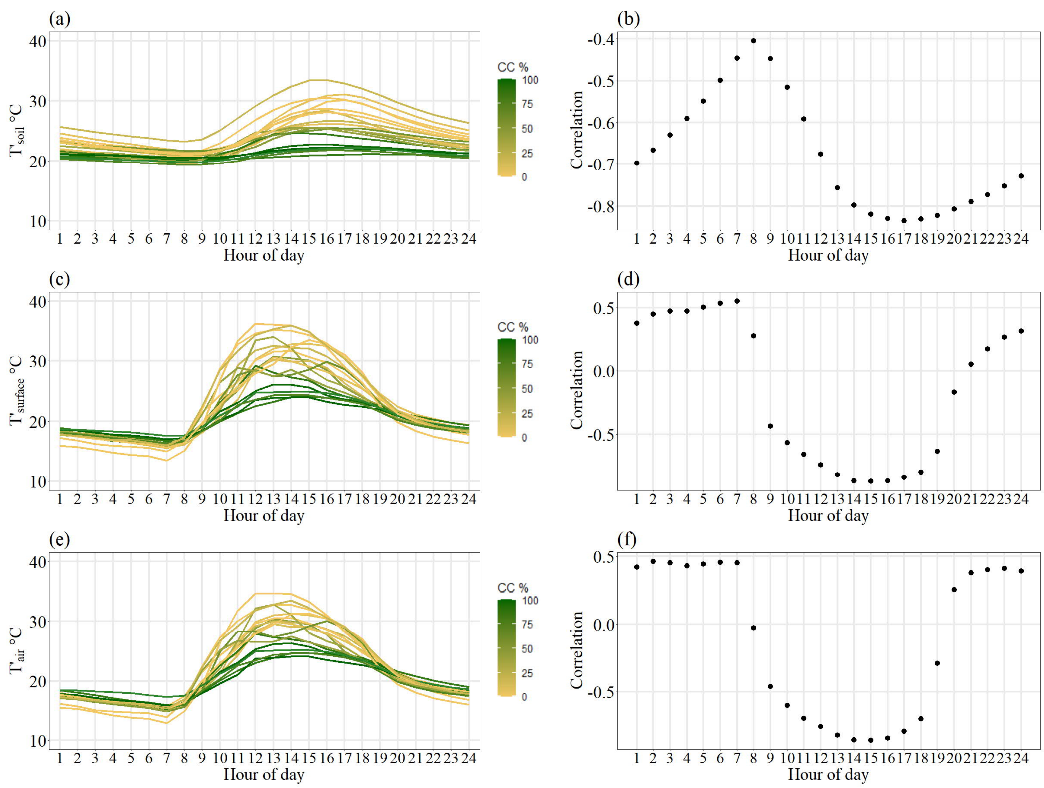

Figure 4: Topographically corrected diurnal mean temperatures (T') (left) and the correlation between T' and canopy cover (CC) percentage (right) between June 13 and July 10, 2019. Hour refers to ordinal number of hour, e.g. 1 means 00:00–01:00. Line color indicates CC percentage. a–b) Soil temperature. c–d) Surface temperature. e–f) Air temperature.

3.1.2 Mean, maximum and minimum temperatures

Mean temperatures had significant negative correlation with CC at all the measurement heights ($T'_{surface}$ and T'_{air} r = -0.84, T'_{soil} r = -0.78). Based on the linear regression, an increase from 0% to 100% CC decreased T'_{soil} by 5.2 °C (R^2 =

https://doi.org/10.5194/bg-2021-261
Preprint. Discussion started: 21 October 2021

0.6), $T'_{surface}$ by 5.9 °C (R^2 = 0.71) and T'_{air} by 4.6 °C (R^2 = 0.71) (Fig. 5). The average effect on combined T'_{soil}, $T'_{surface}$ and T'_{air} was 5.7 °C (R^2 = 0.65). $T'_{surface}$ and T'_{air} were in general higher than T'_{soil}, which was a case also with temperature maxima.

CC had a strong effect on maximum temperatures at all measurement heights, $T'_{surface}$ being affected the most. High CC sites experienced the lowest $T'_{surface}$ and T'_{air} maxima, while $T'_{surface}$ and T'_{air} were the hottest in Maktau and sites with zero % CC. Here, average maximum temperatures ranged between 30 °C and 38.5 °C. The linear models showed that the increase from zero % CC to 100% CC decreased the maximum T'_{soil} by 9 °C (R^2 = 0.69), $T'_{surface}$ by 12.1 °C (R^2 = 0.74) and T'_{air} by 9.6 °C (R^2 = 0.69) (Table 3). On average, the difference was 10.2 °C. Based on the model coefficients, which indicate the magnitude of the influence of CC on temperature, the cooling effect of CC was stronger on maximum T'_{soil} and $T'_{surface}$ than mean, while CC affected T'_{air} mean more than maximum.

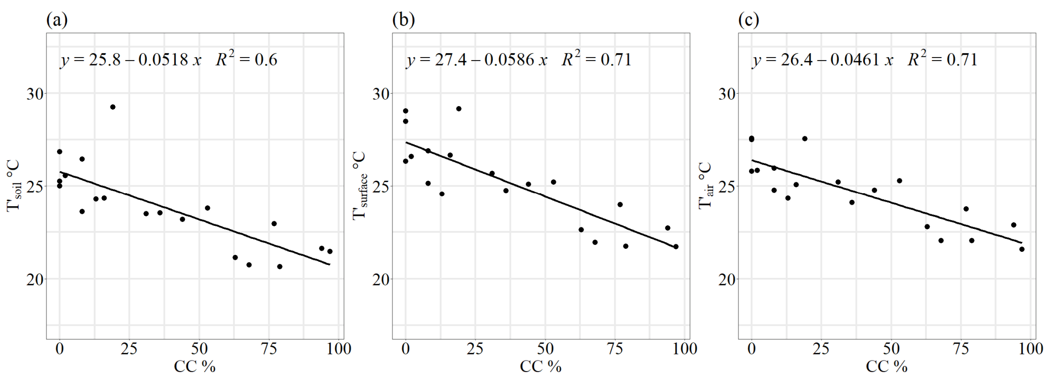

Figure 5: Scatterplots of topographically corrected daytime mean temperatures (T') against canopy cover (CC) percentage, with regression line. a) Soil temperature. b) Surface temperature. c) Air temperature.

Minimum temperatures showed no explicit relationship with CC, and sites with similar CC% had high temperature variability. R^2 were low (< 0.2) at all measurement heights, and correlations between temperatures and CC were insignificant.

https://doi.org/10.5194/bg-2021-261
Preprint. Discussion started: 21 October 2021

	Measurement height	Max (C°)	Site, CC %	Min (C°)	Site, CC %	Coef	R^2	r	p-value
Mean	T'_{soil}	29.3	Maktau, 19 %	20.6	Bura river, 79 %	-0.052	0.604	-0.777	<0.001*
	$T'_{surface}$	29.2	Maktau, 19 %	21.7	Chawia, 97 %	-0.059	0.711	-0.843	<0.001*
	T'_{air}	27.6	Sarova 2, 0 %	21.6	Chawia, 97 %	-0.046	0.710	-0.842	<0.001*
Maximum	T'_{soil}	33.3	Maktau, 19 %	20.8	Bura river,79 %	-0.09	0.693	-0.832	<0.001*
	$T'_{surface}$	38.8	Sarova 2, 0 %	22.9	Chawia ,97 %	-0.121	0.742	-0.862	<0.001*
	T'_{air}	37.4	Sarova 2, 0 %	23.8	Chawia, 97 %	-0.1	0.686	-0.828	<0.001*
Minimum	T'_{soil}	23.0	Maktau, 19 %	19.2	Bura, 68 %	-0.003	0.083	-0.289	0.231
	$T'_{surface}$	19.5	Chawia, 97 %	12.9	Sarova 2, 0 %	-0.024	0.189	0.435	0.063
	T'_{air}	19.3	Ngangao 2, 77 %	12.3	Sarova 2, 0 %	-0.023	0.149	0.386	0.102

Table 3. Topographically corrected temperature (T') statistics for the soil, surface and air. Temperatures in the maximum and minimum columns refer to the highest and lowest mean, maximum and minimum temperatures. Site refers to where the highest and lowest temperatures were measured and their respective canopy cover (CC) percentage. * indicates statistical significance.

3.2 Landsat 8 Land surface temperature

3.2.1 Land surface temperature compared with temperatures measured in the field

LST and raw field temperatures (T) at the time of satellite overpass showed statistically significant correlation (*r* = 0.82, 0.79 and 0.84 at T_{soil}, $T_{surface}$ and T_{air}, respectively) (Fig. 6). At 18 sites out of 19, LST was higher than T_{soil}, whereas between LST and $T_{surface}$ or T_{air} there was no consistent difference. Mean differences were 4.1 °C (T_{soil}), -0.03 °C ($T_{surface}$) and 0.57 °C (T_{air}). The T_{soil} difference was statistically significant with 95 % confidence, while $T_{surface}$ and T_{air} not.

https://doi.org/10.5194/bg-2021-261
Preprint. Discussion started: 21 October 2021

Biogeosciences
Discussions
Open Access

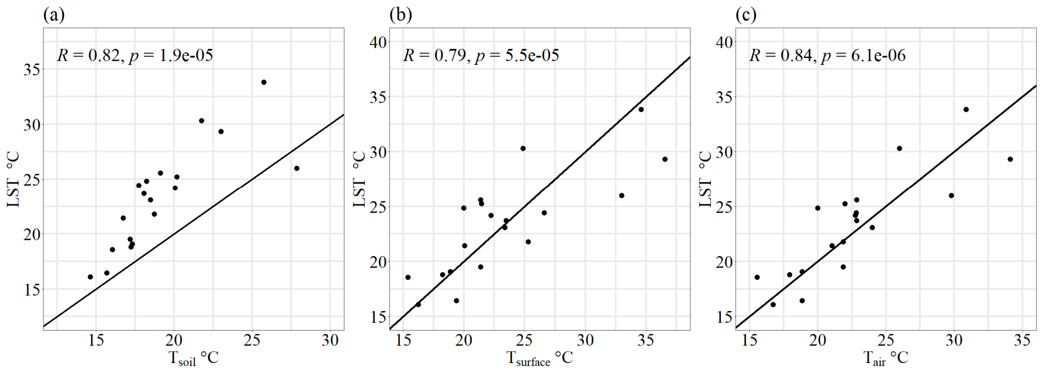

Figure 6: Landsat 8 land surface temperature (LST) compared with raw field temperatures (T) at the time of satellite overpass (10:30) on July 4, 2019. a) LST and soil temperature. b) LST and surface temperature. c) LST and air temperature.

3.2.2 Impact of canopy cover on land surface temperature

All the variables in Model 1 showed statistical significance (R^2 = 0.74). Based on the regression analysis, generally the increase from zero % CC to 100% CC decreased LST with 5 °C (Table 4). After the exclusion of other variables except CC, correlation between LST and CC was -0.37 ($p < 0.001$) and R^2 = 0.14. Topographic correction based on Model 1 improved the correlation coefficient to -0.42 and R^2 to 0.18.

In Model 2, three elevation zones were added to the model. This increased the R^2 to 0.77, demonstrating a notable difference in the cooling effect of CC depending on elevation zone. At the elevations below 1000 m, the cooling effect of CC when moving from zero % CC to 100% CC was -6.6 °C, between 1000–1500 m the effect was -3.2 °C, and above 1500 m the effect was -2.8 °C (Table 4). Roughly, the cooling impact of CC was about a half in the hills compared to the effect in the lowlands.

In Model 3, the interaction term of CC and elevation zones was replaced with interaction term of CC and the continuous variable elevation from the DEM. This produced R^2 = 0.74. The coefficient for the interaction term was 0.00005, indicating that increase of 1000 m in elevation decreased the cooling effect of CC by 0.05 °C (Table 4). The model performed poorer compared to Model 2.

Model 4 was built up on Model 2 by adding interaction terms between aspect classes and CC (Table 4). According to the results from Model 4, the magnitude of aspect's influence on the cooling effect of CC was mostly insignificantly small,

https://doi.org/10.5194/bg-2021-261
Preprint. Discussion started: 21 October 2021

Biogeosciences Discussions
Open Access
EGU

except in the cases of north-east, east and south-east, where the coefficients decreased by roughly 0.01 °C. Model 4 performed best of the four (R^2 = 0.77).

In summary, including either of the elevation factors (DEM or elevation zones) in the model showed that elevation affected CC's cooling effect significantly, having two times higher impact in the lowlands compared to the hills. The dependence of CC's impact on elevation is demonstrated in Fig. 7 using eight elevation classes. CC's coefficients decreased with increasing elevation after 1000 m, yet increased again between 1200–1400 m to roughly the same as in the lowlands. The effect was the smallest in elevations above 1800 m.

Predictor	Model	Coef	Std. Error	T-Value	P-Value
Constant	1	44.79	0.013	3324.0	<0.001*
	2	44.24	0.019	2300.9	<0.001*
	3	46.71	0.018	2580.3	<0.001*
	4	44.38	0.021	2142.5	<0.001*
Elevation	1	-0.013	0.000	-1241.4	<0.001*
	2	-0.011	0.000	-577.2	<0.001*
	3	-0.015	0.000	-954.6	<0.001*
	4	-0.011	0.000	-579.3	<0.001*
Slope	1	-4.061	0.018	-220.0	<0.001*
	2	-3.806	0.018	-214.9	<0.001*
	3	-3.723	0.018	-202.3	<0.001*
	4	-3.781	0.018	-212.6	<0.001*
Canopy cover	1	-0.050	0.000	-419.0	<0.001*
	2	-0.068	0.000	-449.1	<0.001*
	3	-0.109	0.000	-274.7	<0.001*
	4	-0.073	0.000	-208.0	<0.001*
NE	1	0.177	0.011	16.0	<0.001*
	2	0.084	0.010	8.1	<0.001*
	3	0.157	0.011	14.3	<0.001*
	4	-0.215	-0.015	-14.0	<0.001*

E	1	-0.030	0.010	-29.0	<0.001*
	2	-0.428	0.010	-44.6	<0.001*
	3	-0.352	0.010	-34.7	<0.001*
	4	-0.766	0.014	-55.2	<0.001*
SE	1	-1.447	0.010	-140.0	<0.001*
	2	-1.509	0.010	-155.6	<0.001*
	3	-1.529	0.010	-149.3	<0.001*
	4	-1.733	0.014	-127.3	<0.001*
S	1	-2.095	0.011	-189.4	<0.001*
	2	-2.132	0.010	-205.2	<0.001*
	3	-2.186	0.011	-199.4	<0.001*
	4	-2.166	0.014	-153.3	<0.001*
SW	1	-2.441	0.011	-230.0	<0.001*
	2	-2.554	0.010	-256.0	<0.001*
	3	-2.527	0.011	-240.1	<0.001*
	4	-2.538	0.014	-185.9	<0.001*
W	1	-2.293	0.010	-219.5	<0.001*
	2	-2.254	0.010	-229.9	<0.001*
	3	-2.332	0.010	-225.5	<0.001*
	4	-2.195	0.014	-159.0	<0.001*
NW	1	-1.380	0.011	-126.8	<0.001*
	2	-1.205	0.010	-117.9	<0.001*
	3	-1.379	0.012	-127.9	<0.001*
	4	-1.196	0.015	-81.9	<0.001*
1000-1500 m	1	.	.	.	.
	2	-2.667	0.008	-346.9	<0.001*
	3	.	.	.	.
	4	-2.678	0.008	-348.5	<0.001*
>1500 m	1	.	.	.	.

https://doi.org/10.5194/bg-2021-261
Preprint. Discussion started: 21 October 2021

	2	-2.030	0.018	-111.2	<0.001*
	3	.	.	.	.
	4	-2.006	0.018	-110.0	<0.001*
Canopy cover: 1000–1500 m	1	.	.	.	.
	2	0.031	0.000	149.7	<0.001*
	3	.	.	.	.
	4	0.032	0.000	153.5	<0.001*
Canopy cover: >1500m	1	.	.	.	.
	2	0.028	0.000	120.7	<0.001*
	3	.	.	.	.
	4	0.038	0.000	121.6	<0.001*
Elevation: canopy cover	1	.	.	.	.
	2	.	.	.	.
	3	0.00005	0.000	156.3	<0.001*
	4	.	.	.	.
Canopy cover: NE	1	.	.	.	.
	2	.	.	.	.
	3	.	.	.	.
	4	0.011	0.000	25.6	<0.001*
Canopy cover: E	1	.	.	.	.
	2	.	.	.	.
	3	.	.	.	.
	4	0.013	0.000	32.6	<0.001*
Canopy cover: SE	1	.	.	.	.
	2	.	.	.	.
	3	.	.	.	.
	4	0.010	0.000	24.0	<0.001*
Canopy cover: S	1	.	.	.	.
	2	.	.	.	.

	3	.	.	.	.
	4	-0.000	0.000	-0.2	0.8
Canopy cover: SW	1	.	.	.	.
	2	.	.	.	.
	3	.	.	.	.
	4	-0.003	0.000	-8.0	<0.001*
Canopy cover: W	1	.	.	.	.
	2	.	.	.	.
	3	.	.	.	.
	4	-0.003	0.000	-7.8	<0.001*
Canopy cover: NW	1	.	.	.	.
	2	.	.	.	.
	3	.	.	.	.
	4	-0.000	0.000	-1.2	0.25

Table 4: Summary of regression coefficients in the analysis of land surface temperature (LST) from the four models tested. * indicates statistical significance.

https://doi.org/10.5194/bg-2021-261
Preprint. Discussion started: 21 October 2021

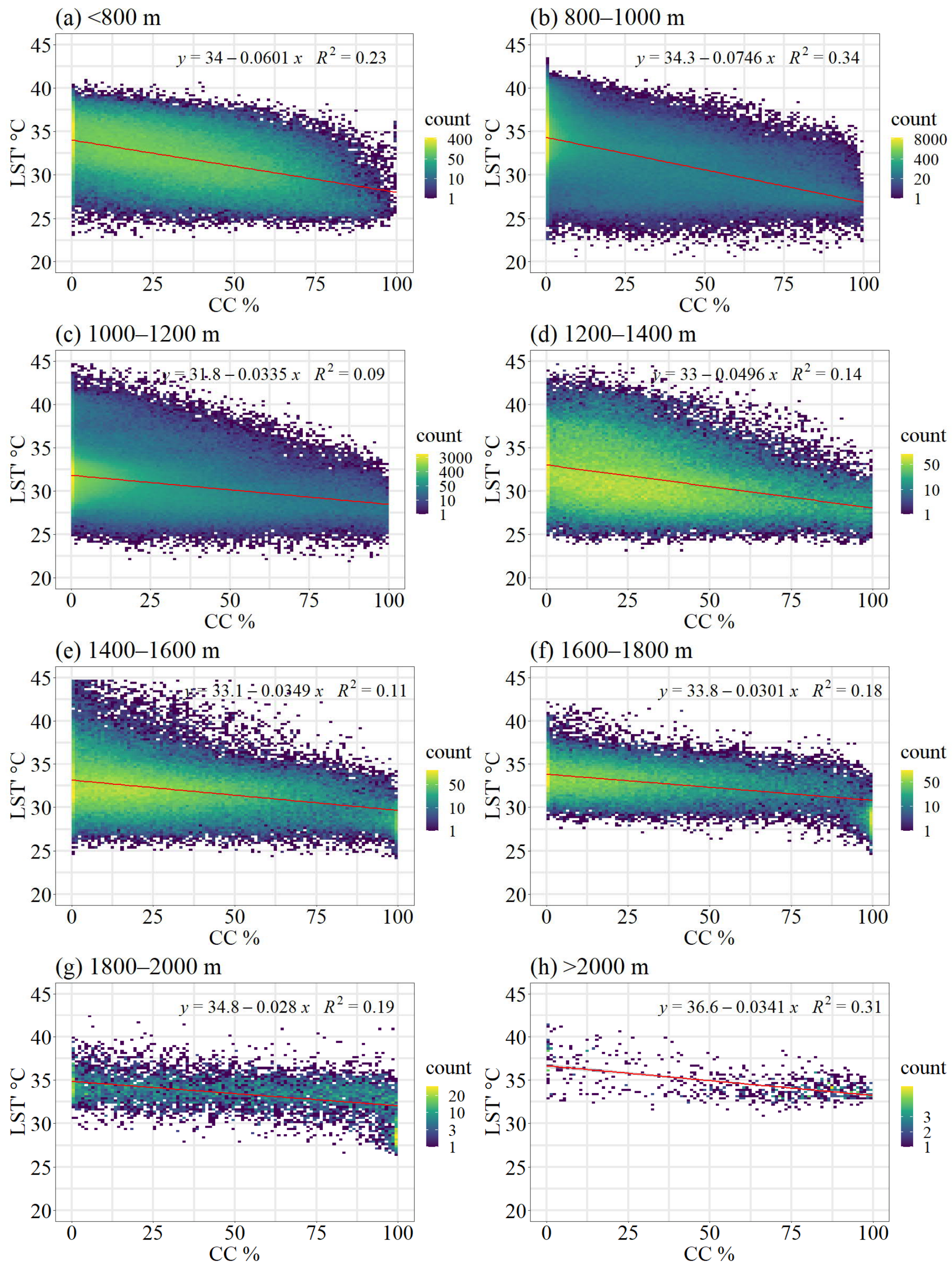

Figure 7: Density plots of topographically corrected land surface temperature (LST') and canopy cover (CC) percentage in eight elevation classes, with regression line. a) below 800 m. b) 800–1000 m. c) 1000–1200 m. d) 1200–1400 m. e) 1400–1600 m. f) 1600–1800 m. g) 1800–2000 m. h) above 2000 m.

4. Discussion

High CC decreased near-ground mean temperatures on average by 5.7 °C compared to open land, depending on measurement height. The difference was even greater in temperature maxima, which has been reported to be the case also by De Frenne et al. (2019) and Belsky et al. (1989). Temperature and CC had a linear relationship, pointing out that closed CC was not needed for a sensible cooling effect. $T_{surface}$ was affected the most by CC. Despite the measurement height of $T_{surface}$ being only 13 cm below T_{air}, the effect of CC was notably weaker in T_{air}, which is in line with previous studies. For example, Luyssaert et al. (2014) report that the temperature of the planetary boundary was less affected than LST by the removal of forest cover, while in De Frenne et al. (2019) temperature offset between forest and open land was the greatest close to the ground. In Belsky et al. (1989), soil temperature was the least affected by CC.

The prevalent temperatures affected the magnitude of the cooling: in elevations above 1000 m, the cooling effect decreased remarkably by approximately 50 % compared to the lowlands. Moreover, based on the temporal data from the microclimate sensors, during the cooler days of overcast conditions, CC's cooling effect was smaller. Additionally, the temperature differences between low and high CC sites were smaller during these days. One likely reason behind the phenomenon is that plant evapotranspiration rates are relative to the solar radiation and ambient temperatures (Allen et al. 1998). It can be concluded that trees' importance in controlling temperatures increases in hotter environments. The discovery is meaningful, since agricultural expansion on the cost of woody vegetation cover in the area is predicted to take place predominantly in the lowlands (Erdogan et al. 2011; Maeda et al., 2010), where the temperatures are very high. Increasing tree cover on farmlands could thus be of considerable benefit in decreasing local temperatures.

The impact of CC on temperature is also most likely different on different days and different times of the year. For instance, Maeda and Hurskainen (2014) found that land cover's influence on LST in Mount Kilimanjaro varied seasonally and diurnally, and the effect was dependent on elevation. Our LST estimation using the satellite image was only a snapshot for July 4, 2019, from a sunny almost cloud-free day, and does not represent the year-round situation experiencing two rainy seasons, which are cloudy. In the hills, cloudy and misty conditions are experienced throughout the year (Helle, 2016; Räsänen et al., 2018). A time series comparing the cooling effect of CC over seasons and several years is an interesting future research topic, as the TOMST sensors remained in the 19 field plots. Interesting would also be to model the sunshine hours every day in the locations of the TOMST sensors using the hemispherical photography, in order to assess how many hours of the day the tree cover causes shadows on the sensor.

The thermal environments of forests are controlled by canopies to a high extent, which was reaffirmed in this study. Therefore, CC can mitigate large-scale macroclimate warming (De Frenne et al., 2019). An increase of 2 °C of the global temperature as a consequence of enhanced greenhouse effect can have detrimental impacts on the most vulnerable ecosystems (IPCC, 2018). Since the time span of local changes in temperatures due to LULCC is much shorter than in the global climate change, the regional and local consequences can be of even higher extent (Chen et al., 1999). Due to the debts of species' adaptation capabilities to climate warming (Zellweger et al., 2020), changes in the microclimate temperatures may be fatal for flora and fauna occupying narrow thermal niches. This may further impact biodiversity and consequently the crucial ecosystem services provided by forests that take place close to ground surface (Chen, et al. 1999; Zellweger et al., 2020).

Forest fragmentation decreases the ability of tropical forest to mitigate climate change (Ewers and Banks-Leite, 2013), but on regional scale even small forests have an impact on LST (Mildrexler et al., 2011). Our results revealed that trees on farms had the same effect on local temperatures as forests despite the smaller scale, and could hence help in conserving the biodiversity. For instance, Mendenhall et al. (2016) found that in Costa Rica farm trees increased the number of tree and plant species. Most of the CC in Taita Hills comprises of TOF, occurring on farms and human settlement. Sites with agroforestry trees and moderate CC were already experiencing both lower mean and maximum temperatures than the open sites.

In Taita Hills, Pellikka et al. (2018) reported an addition in carbon stocks since 2003. The Agriculture (Farm Forestry) Rules of 2009 requires that at least 10 % forest cover should be left or planted on farms. Based on our results, this 10 % CC makes a significant difference in temperatures. Soil and air temperatures have an impact to crop productivity, and furthermore, the fog deposit captured by trees brings more water to plants. In general, increasing temperatures make plant growth more efficient, but this is the case only as long as the increase occurs within the thermal limits of the plant's tolerance (Muimba-Kankolongo, 2018). As extreme heat and precipitation events are becoming more common with climate change (MoALF, 2016; IPCC, 2018), the negative effects of warming will become notable in sub-Saharan Africa. This further threatens the food security, and especially the most common crop, maize, which is one of the most vulnerable crops in terms of climate change in Africa (Cairns et al., 2013; Adhikari et al., 2015). Forests of Taita Hills contribute to the food security by capturing atmospheric moisture as fog deposit and storing the water providing water for farms in the foothills and lowlands (Pellikka et al., 2013; Helle, 2016).

The pressure on tropical forests in sub-Saharan Africa is caused by many reasons, fuelwood collection being significant (Abdelgalil, 2004), which could be mitigated by increasing the tree cover on farms (Unruh et al., 1993). The results of this study further encourage to increase tree cover in particular in the lowland farms as a strong potential way to fight the negative effects of climate change. Nevertheless, water is scarce especially in the lowland areas, and trees' vast need for water must be taken into account. The phenomenon is paradoxical, since trees improve the water cycle, in general, but are consumes high amounts of water (Ong et al., 2006). In areas with water scarcity, the competition of water resources with crops, animals and people may be a limiting factor in the adoption of agroforestry practices. One solution in the hot lowlands is dew collection, but it would require a tree cover or other surfaces to capture the humidity. In Tuure et al. (2019), artificial surfaces produced at best 0.1 liter per day and 25 liters in a year water from morning dew.

This study was limited to a short time span and a small sample size in microclimate study sites, which makes it susceptible for uncertainties associated with temporal and spatial variability. Topographic correction was applied on the microclimate data and was calculated based on elevation only. The small amount of observations did not allow for calculation the impact of the aspect, which is expected to exist based on the LST analysis. Due to the topographic manipulation of the temperatures, they did not represent the true values recorded, but made the temperatures comparable by CC. In terms of LST, as has been documented in several studies, spaceborne TIR remains an uncertain method for accurate LST retrieval (Simó et al., 2018; Li et al., 2013). After all, LST is an indirect measurement and the results of complicated mathematical processing requiring knowledge of several components, where error in any of them causes inaccuracies in LST (Simó et al., 2018). Estimation of land surface emissivity is determinant in the correct LST retrieval, yet highly difficult to measure and prone to error. Moreover, in dense canopies the signal constitutes mostly of the upper canopy and does not necessarily capture the temperatures on the forest floor, which may not make LST representative of understory conditions (Bense et al., 2016; Zellweger et al., 2019). Landsat 8 TIRS band 11 was not used in this study due to the stray light problem, which exposes even higher possibility of inaccuracy with LST. However, Wang et al. (2019) conclude that the SC is a valid method for Landsat 8 processing and produces results on accuracy high enough for most purposes.

Despite its limitations, this study provided information about a topic of which importance has only recently been recognized (De Frenne et al., 2013; Jucker et al., 2018; Zellweger et al., 2020). Research and modelling of climate change implications on microclimate cannot rely on observations from weather stations with low spatial resolution, but need data that represent the microclimatic conditions relevant for most ecosystem functions. Previous research about vegetation and LST have been often conducted at much lower spatial resolutions and applied less accurate topographic correction (Li et al., 2015). Furthermore, the effect of trees on climate is usually studied solely based on comparison between forest and open land (De Frenne et al., 2019), neglecting the intermediate canopies and their significance, despite of the fact that human activity focuses mostly in areas with TOF. We used microclimate data covering a CC gradient and satellite-derived LST data combined with a DEM of 30 m acquired with ALS over the versatile and precise study area. While establishing

https://doi.org/10.5194/bg-2021-261
Preprint. Discussion started: 21 October 2021

Biogeosciences Discussions
Open Access

field observation networks with wide spatial coverage remains a challenge, our results showed that LST can be used as a proxy for assessing the impacts of CC on microclimate.

Future research should further investigate the contribution of varied factors to microclimate. For example, since all trees are not of equal benefits in agroforestry, more studies could be targeted to the comparison of different agroforestry species' cooling potential as well as the potential of plantation forests. Including soil moisture, air temperature and comprehensive field plot networks under different canopy structures in the future analyses should broaden the knowledge about trees' role in mitigating and adapting to climate change.

5. Conclusions

Our results demonstrate a consistent but heterogeneous influence of canopy cover on the microclimate of highly diverse tropical ecosystems. Daytime temperatures correlated inversely with canopy cover, the effect being strongest on surface temperatures. During the hottest days, the difference between sites of high and low canopy cover became most notable. The cooling effect did not exist only with high canopy cover, but even intermediate canopy cover and trees outside forest buffered the hottest temperatures. Our results thus provide robust evidence that any efforts in the direction of preserving, restoring or increasing vegetation cover can have a substantial impact in creating more stable and cooler microclimates. Satellite based LST was a suitable proxy for assessing microclimatic variables surface- and near-ground temperatures, particularly in heterogeneous regions, where the network of field measurements cannot cover the spatial microclimate variability.

This study provided valuable information about the potential of trees in climate change adaptation and mitigation in tropical environments. As the effect of canopy cover on microclimate increased at lower elevations and during hot days, our results indicate that warmer and drier regions are likely to benefit the most from trees.

https://doi.org/10.5194/bg-2021-261
Preprint. Discussion started: 21 October 2021

Appendix A. Method for hemispherical photography

We took hemispherical photographs at every microclimate sensor site. The camera in use was Nikon D5000 DSLR and the lens Sigma 4.5 mm F2.8 EX DC HSM Circular Fisheye. The camera was attached to a tripod during the taking of photographs. We took photographs at two different heights: the lowest possible tripod adjustment to be as close to the actual sensor level as possible, which was around 60 cm, and at eye-level around 130 cm. We took photographs at eye-level also to every intercardinal direction 15 meters away from the sensor. The camera was adjusted looking upward with the top of the camera pointing north. Two images at every height and direction were taken with different settings: first image on Program mode with automatic aperture and shutter speed, and the second on Manual mode with the rest of the settings staying the same as in picture one, except shutter speed was reduced to half of the first mage. The ISO value was set as constant 500. The purpose of the smaller shutter speed was to reduce the impact of light conditions that were not optimal, meaning direct sunlight that causes overexposure of images which in turn makes them difficult to analyze. Optimally, the photographs should be taken under constant cloud cover or at the dawn or dusk (Pellikka et al., 2000), however due to the timetable, waiting for better light conditions at some sites was not possible, thus some images were overexposed.

We analyzed the hemispherical photographs in the software Hemisfer (WSL; version 2.2) (Schleppi et al., 2007; Thimonier et al., 2010). From the two images, we used the less exposed one in the analysis. For the calculation of canopy cover, we used the images taken from eye-level, because they were more comparable to the ALS-based canopy cover, and the photographs in cardinal directions were all taken at eye-level. We classified the image pixels to sky and canopy by determining a threshold value to separate dark and light pixels in the image. For most images, we used the automatic threshold method by Nobis and Hunziker (2005). In the case of some images, the algorithm clearly produced errors due to overexposure and direct sunlight, therefore the algorithm by Ridler and Calvart (1978) was applied, or a manual threshold was determined. We used only the blue band in the analysis, apart from photographs where the classification was failing and using all the bands produced the best result (Heiskanen et al., 2015a). The gamma correction was $\gamma = 2.2$. Only the zenith angle range of 0-15° was analyzed, because errors in canopy cover accuracy increase with larger angles (Paletto and Tosi, 2009). We computed canopy cover by calculating an average of 1-gap fraction of the five measurements, and this gave a plot-wise canopy cover (Heiskanen, et al., 2015b). Finally, we compared the canopy cover retrieved from hemispherical photography and ALS using Pearson's correlation and a Student's t-test.

Data and code availability

The data and scripts presented in this study are available on request from the author (I.A.).

Author contribution

Conceptualization, I.A., E.M., J.H. and P.P.; data curation, I.A.; formal analysis, I.A., E.A.; funding acquisition, P.P.; investigation, I.A., methodology, I.A, E.M., J.H., E.A. and P.P.; project administration, E.M. and P.P.; resources, software, I.A.; supervision, E.M, J.H. and P.P.; validation, I.A., visualization, I.A., writing—original draft preparation, I.A.; writing—review and editing, IA., E.M., J.H. and P.P. All authors have read and agreed to the published version of the manuscript.

Declaration of Competing Interest

The authors declare that they have no conflicts of interest.

Funding

This study was conducted as part of Smartland project (Environmental sensing of ecosystem services for developing a climate-smart landscape framework to improve food security in East Africa, decision no. 31864) funded by Academy of Finland, and ESSA project (Earth observation and environmental sensing for climate-smart sustainable agropastoral ecosystem transformation in East Africa) funded by European Commission DG International Partnerships DeSIRA programme (FOOD/2020/418-132). Eduardo Maeda was funded by the Academy of Finland (decision numbers 318252 and 319905).

Acknowledgements

We would like to acknowledge Agnes Mwangombe, Ali Ndizi, Mrs. Mwamburis, Mrs. Nyatta, Cathrine Mwakesi, Simon, Moses Onyimbo and Dalmas moka secondary school, Jason Collette and Teita Sisal Estate, St. Mary's Teachers' Training College, and Taita Taveta University Ngerenyi campus for allowing us to conduct this research on their properties. We also thank Taita Research Station of the University of Helsinki for logistical support during the field wok campaign. Special thanks to Mwadime Mjomba for assistance during the field work. We acknowledge Matti Räsänen for the provision of weather station data and Hari Adhikari for the canopy cover data.

https://doi.org/10.5194/bg-2021-261
Preprint. Discussion started: 21 October 2021

References

Abdelgalil, E. A.: Deforestation in the drylands of Africa: Quantitative modelling approach, Environment, Development and Sustainability, 6, 415–427, http://dx.doi.org/10.1007/s10668-005-0787-1, 2004.

Abera, T. A., Heiskanen, J., Pellikka, P. K., Adhikari, H., and Maeda, E. E.: Climatic impacts of bushland to cropland conversion in Eastern Africa, Sci. Total. Environ., 717, https://doi.org/10.1016/j.scitotenv.2020.137255, 2020.

Adhikari, H., Heiskanen, J., Siljander, M., Maeda, E., Heikinheimo, V., and Pellikka, P. K.: Determinants of Aboveground Biomass across an Afromontane Landscape Mosaic in Kenya, Remote Sens., 9, 827, https://doi.org/10.3390/rs9080827, 2017.

Adhikari, U., Nejadhashemi, A. P., and Woznicki, S. A.: Climate change and eastern Africa: a review of impact on major crops, Food and Energy Security, 4, 110–132. http://dx.doi.org./10.1002/fes3.61, 2015.

Agriculture (Farm Forestry) Rules, 2009 (Cap. 318) (KEN).

Allen, R. G., Pereira, L. S., Raes, D., and Smith, M.: Crop evapotranspiration - Guidelines for computing crop water requirements, Food and Agriculture Organization of the United Nations, Rome, Italy, 1998

Amara, E., Adhikari, H., Heiskanen, J., Siljander, M., Munyao, M., Omondi, P., and Pellikka, P.: Aboveground Biomass Distribution in a Multi-Use Savannah Landscape in Southeastern Kenya: Impact of Land Use and Fences, Land, 9, 381, https://doi.org/10.3390/land9100381, 2020.

Beer, C., Reichstein, M., Tomelleri, E., Ciais, P., Jung, M., Carvalhais, N., . . . Papale, D.: Terrestrial Gross Carbon Dioxide Uptake Distribution and Covariation with Climate, Science, 329, 834–838, https://doi.org/10.1126/science.1184984, 2010.

Belsky, A. J., Amundson, R. G., Duxbury, J. M., Riha, S. J., Ali, A. R., and Mwonga, S. M.: The Effects of Trees on Their Physical, Chemical and Biological Environments in a Semi-Arid Savanna in Kenya, J. Appl. Ecol., 26, 1005–1024. https://doi.org/10.2307/2403708, 1989.

Bense, V. F., Read, T., and Verhoef, A.: Using distributed temperature sensing to monitor field scale dynamics of ground surface temperature and related substrate heat flux, Agr. Forest. Meteorol., 220, 207–215. https://doi.org/10.1016/j.agrformet.2016.01.138, 2016.

Cairns, J. E., Hellin, J., Sonder, K., Araus, J. L., MacRoberts, J. F., Thierfelder, C., and Prasanna, B. M.: Adapting maize production to climate change in sub-Saharan Africa, Food Secur., 5, 345–360, https://doi.org/10.1007/s12571-013-0256-x, 2013.

Chen, J., Saunders, S. C., Crow, T. R., and Naiman, R. J.: Microclimate in forest ecosystem and landscape ecology, Bioscience, 49, 288–297, http://dx.doi.org/10.2307/1313612, 1999.

Das, A., Nagendra, H., Anand, M., and Bunyan, M.: Topographic and Bioclimatic Determinants of the Occurrence of Forest and Grassland in Tropical Montane Forest-Grassland Mosaics of the Western Ghats, India, PLoS One, 10, e0130566, http://dx.doi.org/10.1371/journal.pone.0130566, 2015.

De Frenne, P., Rodríguez-Sánchez, F., Coomes, D. A., Baeten, L., Verstraeten, G., Vellend, M., . . . Verheyen, K.: Microclimate moderates plant responses to macroclimate warming, P. Natl. Acad. Sci. USA., 110, 18561–18565, https://doi.org./10.1073/pnas.1311190110, 2013.

De Frenne, P., Zellweger, F., Rodríguez-Sánchez, F., Scheffers, B. R., Hylander, K., Luoto, M., . . . Lenoir, J.: Global buffering of temperatures under forest canopies, Nat. Ecol. Evol., 3, 744–749, http://dx.doi.org/10.1038/s41559-019-0842-1, 2019.

Ellison, D., Morris, C. E., Locatelli, B., Sheil, D., Cohen, J., Murdiyarso, D., . . . Sullivan, C. A.: Trees, forests and water: Cool insights for a hot world, Global Environ. Chang., 43, 51–61, https://doi.org/10.1016/j.gloenvcha.2017.01.002, 2017.

Erdogan, H. E., Pellikka, P. K., and Clark, B.: Modelling the impact of land-cover change on potential soil loss in the Taita Hills, Kenya, between 1987 and 2003 using remote-sensing and geospatial data, Int. J. Remote Sens., 32, 5919–5945, https://doi-org.libproxy.helsinki.fi/10.1080/01431161.2010.499379, 2011.

Ewers, R. M., and Banks-Leite, C.: Fragmentation Impairs the Microclimate Buffering Effect of Tropical Forests, PLoS One, 8, e58093, https://doi.org/10.1371/journal.pone.0058093, 2013.

FAO: Global Forest Resources Assessment 2000 (FRA 2000). Food and Agriculture Organization of the United Nations, Rome, Italy, 2000.

FAO: Forest Resources Assessment. Terms and definitions. Food and Agriculture Organization of the United Nations, Rome, Italy, 2015.

FAO: Global forest resources assessment 2015. How are the world's forests changing? (2 ed.), Food and Agriculture Organization of the United Nations, Rome, Italy, 2016.

https://doi.org/10.5194/bg-2021-261
Preprint. Discussion started: 21 October 2021

Griffin, A. M., Popescu, S. C., and Zhao, K.: Using LIDAR and Normalized Difference Vegetation Index to remotely determine LAI and percent canopy cover, in: SilviLaser, Edinburgh, United Kingdom, 17–19 September, 446–455, 2008.

He, J., Zhao, W., Li, A., Wen, F., and Yu, D.: The impact of the terrain effect on land surface temperature variation based on Landsat-8 observations in mountainous areas, Int. J. Remote Sens., 40, 1808–1827, https://doi,org/10.1080/01431161.2018.1466082, 2019.

Heiskanen, J., Korhonen, L., Hietanen, J., and Pellikka, P. K.: Use of airborne lidar for estimating canopy gap fraction and leaf area index of tropical montane forests, Int. J. Remote Sens., 36, 2569–2583, https://doi.org/10.1080/01431161.2015.1041177, 2015a.

Heiskanen, J., Korhonen, L., Hietanen, J., Heikinheimo, V., Schäfer, E., and Pellikka, P. K. E.: Comparison of field and airborne laser scanning based crown cover estimates across land cover types in Kenya, Int. Arch. Photogramm. Remote Sens. Spatial Inf. Sci., XL-7/W3, 409–415, https://doi.org/10.5194/isprsarchives-XL-7-W3-409-2015, 2015b.

Helle, J.: Lentolaserkeilaus ja hemisfäärikuvaus metsikkösadannan tutkimisessa Taitavuorilla Keniassa, B.Sc. thesis, University of Helsinki, 2016.

IPCC: Global Warming of 1.5°C. An IPCC Special Report on the impacts of global warming of 1.5°C above pre-industrial levels and related global greenhouse gas emission pathways, in the context of strengthening the global response to the threat of climate change, sustainable development, and efforts to eradicate poverty, Intergovernmental Panel on Climate Change, 2018.

Jiménez-Muñoz, J. C., and Sobrino, J. A.: A generalized single-channel method for retrieving land surface temperature from remote sensing data, J. Geophys. Res., 108, 4688, https://doi.org/10.1029/2003JD003480, 2003.

Jiménez-Muñoz, J. C., Sobrino, J. A., Skoković, D., Mattra, C., and Cristóbal, J.: Land Surface Temperature Retrieval Methods from Landsat-8 Thermal Infrared Sensor Data. IEEE Geosci. Remote S., 11, 1840–1843, https://doi.org/10.1109/LGRS.2014.2312032, 2014.

Jin, M., and Dickinson, R. E.: Land surface skin temperature climatology: benefitting from the strengths of satellite observations, Environ. Res. Lett., 5, https://doi.org/10.1088/1748-9326/5/4/044004, 2010.

Jucker, T., Hardwick, S. R., Both, S., Elias, D. D., Ewers, R. M., Milodowski, D. T. . . . Coomes, D. A.: Canopy structure and topography jointly constrain the microclimate of human-modified tropical landscapes, Glob. Change Biol., 24, 5243–5258, https://doi.org/10.1111/gcb.14415, 2018.

https://doi.org/10.5194/bg-2021-261
Preprint. Discussion started: 21 October 2021

Kim, J.-P.: Variation in the accuracy of thermal remote sensing, Int. J. Remote Sens., 34, 729–750, https://doi.org/10.1080/01431161.2012.713143, 2013.

Korhonen, L., Korhonen, K. T., Rautiainen, M., and Stenberg, P.: Estimation of Forest Canopy Cover: A Comparison of Field Measurement Techniques, Silva Fenn., 40, 577–588, https://doi.org/10.14214/sf.315, 2006.

Li, Y., Zhao, M., Motesharrei, S., Mu, Q., Kalnay, E., and Li, S.: Local cooling and warming effects of forests based on satellite observations, Nature Communications, 6, http://dx.doi.org/10.1038/ncomms7603, 2015.

Li, Y., De Noblet-Ducoudré, N., Davin, E. L., Motesharrei, S., Zeng, N., Li, S., and Kalnay, E.: The role of spatial scale and background climate in the latitudinal temperature response to deforestation, Earth Syst. Dynam., 7, 167–181, https://doi.org/10.5194/esd-7-167-2016, 2016.

Li, Z.-L., Tang, B.-H., Wu, H., Ren, H., Yan, G., Wan, Z., . . . Sobrino, J. A.: Satellite-derived land surface temperature: Current status and perspectives. Remote Sens. Environ., 131, 14–37, https://doi.org/10.1016/j.rse.2012.12.008, 2013.

Luyssaert, S., Jammet, M., Stoy, P. C., Estel, S., Pongratz, J., Ceschia, E., . . . Dolman, A. J.: Land management and land-cover change have impacts of similar magnitude on surface temperature, Nat. Clim. Change, 4, 389–393, http://dx.doi.org.libproxy.helsinki.fi/10.1038/nclimate2196, 2014.

Maeda, E. E., and Hurskainen, P.: Spatiotemporal characterization of land surface temperature in Mount Kilimanjaro using satellite data, Theor. Appl. Climatol., 118, 497–509, http://doi.org/10.1007/s00704-013-1082-y, 2014.

Maeda, E. E., Clark, B. J., Pellikka, P., and Siljander, M.: Modelling agricultural expansion in Kenya's Eastern Arc Mountains biodiversity hotspot, Agr. Syst., 103, 609–620, http://dx.doi.org/10.1007/s00704-013-1082-y, 2010.

Martínez Pastur, G., Perera, A. H., Peterson, U., and Iverson, L. R.: Ecosystem Services from Forest Landscapes: An Overview, in: Ecosystem Services from Forest Landscape, edited by: Perera, A., Peterson, U., Pastur, G., and Iverson, L. Springer, https://doi.org/10.1007/978-3-319-74515-2, 2018.

Mendenhall, C. D., Shields-Estrada, A., Krishnaswami, A. J., and Daily, G. C.: Quantifying and sustaining biodiversity in tropical agricultural landscapes, P. Natl. Acad. Sci. USA, 113, 14544–14551, https://doi-org/10.1073/pnas.1604981113, 2016.

Mildrexler, D. J., Zhao, M., and Running, S. W.: A global comparison between station air temperatures and MODIS land surface temperatures reveals the cooling role of forests, J. Geophys. Res., 116, https://doi.org/10.1029/2010JG001486, 2011.

https://doi.org/10.5194/bg-2021-261
Preprint. Discussion started: 21 October 2021

MoALF: Climate Risk Profile for Taita Taveta. Kenya County Climate Risk Profile Series, The Kenya Ministry of Agriculture, Livestock and Fisheries (MoALF), Nairobi, 2016.

Muimba-Kankolongo, A.: Food Crop Production by Smallholder Farmers in Southern Africa, Academic Press, pp. 382, 2018.

Mwalusepo, S., Massawe, E. S., Affognon, H., Okuku, G. O., Kingori, S., Mburu, P. D., . . . Le Ru, B. P.: Smallholder Farmers' Perspectives on Climatic Variability and Adaptation Strategies in East Africa: The Case of Mount Kilimanjaro in Tanzania, Taita and Machakos Hills in Kenya, J. Earth Sci. Clim. Change, 6, http://dx.doi.org/10.4172/2157-7617.1000313, 2015.

Ndossi, M. I., and Avdan, U.: Application of Open Source Coding Technologies in the Production of Land Surface Temperature (LST) Maps from Landsat: A PyQGIS Plugin, Remote Sens., 8, 413. https://doi.org/10.3390/rs8050413, 2016.

Nemani, R., Pierce, L., and Running, S.: Developing Satellite-derived Estimates of Surface Moisture Status, J. Appl. Meteorol., 32, 548–557, 1993.

Ong, C. K., Black, C. R., and Muthuri, C. W.: Modifying forestry and agroforestry to increase water productivity, CAB Reviews: Perspectives in Agriculture, Veterinary Science, Nutrition and Natural Resources, 1, https://doi.org/10.1079/PAVSNNR20061065, 2006.

Pellikka, P., and Hakala, E.: Climate change, in: Megatrends in Africa, edited by: Vastapuu, I., Mattlin, M., Hakala, E., and Pellikka, P., 7–14, Ministry of Foreign Affairs of Finland, 2019.

Pellikka, P. K., Lötjönen, M., Siljander, M., and Lens, L.: Airborne remote sensing of spatiotemporal change (1955–2004) in indigenous and exotic forest cover in the Taita Hills, Kenya, Int. J. Appl. Earth Obs., 11, 221–232, https://doi.org/10.1016/j.jag.2009.02.002, 2009.

Pellikka, P. K., Clark, B. J., Gosa, A. G., Himberg, N., Hurskainen, P., Maeda, E., . . . Siljander, M.: Agricultural Expansion and Its Consequences in the Taita Hills, Kenya, in: Developments in Earth Surface Processes, Vol. 16, edited by: Paron, P., Olago, D., and Omuto, C.T., Elsevier, Amsterdam, 165–179, 2013.

Pellikka, P. K., Heikinheimo, V., Hietanen, J., Schäfer, E., Siljander, M., and Heiskanen, J.: Impact of land cover change on aboveground carbon stocks in Afromontane landscape in Kenya, Appl. Geogr., 94, 178–189, https://doi.org/10.1016/j.apgeog.2018.03.017, 2018.

https://doi.org/10.5194/bg-2021-261
Preprint. Discussion started: 21 October 2021

Biogeosciences Discussions

Potter, K. A., Woods, H. A., and Pincebourde, S.: Microclimatic challenges in global change biology, Glob. Change Biol., 19, 2932–2939, https://doi.org/10.1111/gcb.12257, 2013.

Prata, A. J., Caselles, V., Coll, C., Sobrino, A., and Ottlé, C.: Thermal Remote Sensing of Land Surface Temperature from Satellites: Current Status and Future Prospects, Remote Sensing Reviews, 12, 175–224, https://doi.org/10.1080/02757259509532285, 1995.

R Core Team: RStudio: Integrated Development for R. RStudio, PBC, Boston, United States: http://www.rstudio.com/, 2019.

Räsänen, M., Chung, M., Katurji, M., Pellikka, P., Rinne, J., and Katul, G. G.: Similarity in Fog and Rainfall Intermittency, Geophys. Res. Lett., 45, 10691–10699, 2018.

Simó, G., Martínez-Villagrasa, D., Jiménez, M. A., and Cuxart, J.: Impact of the Surface–Atmosphere Variables on the Relation between Air and Land Surface Temperatures, Pure Appl. Geophys., 175, 3939–3953, https://doi.org/10.1007/s00024-018-1930-x, 2018.

Thijs, K. W., Aerts, R., van der Moortele, P., Aben, J., Musila, W., Pellikka, P., Gulinck, H., and Muys, B.: Trees in a human-modified tropical landscape: Species and trait composition and potential ecosystem services, Landscape Urban Plan., 144, 49–58, https://doi.org/10.1016/j.landurbplan.2015.07.015, 2015.

Tuure, J., Korpela, A., Hautala, M., Hakojärvi, M., Mikkola, H., Räsänen, M., Duplissy, J., Pellikka, P., Kulmala, M., Petäjä, T., and Alakukku, L.: Comparison of surface foil materials and dew collectors location in an arid area: a one-year experiment in Kenya, Agr. Forest Meteorol. 276–277, 107613, https://doi.org/10.1016/j.agrformet.2019.06.012, 2019.

Unruh, J. D., Houghton, R. A., and Lefebvre, P. A.: Carbon storage in agroforestry: an estimate for sub-Saharan Africa, Clim. Res., 3, 39–52, 1993.

USGS. (2017). Landsat 8 OLI and TIRS Calibration Notices: https://www.usgs.gov/land-resources/nli/landsat/landsat-8-oli-and-tirs-calibration-notices, last access: 17 February 2020, 2017.

Wachiye, S., Merbold, L., Vesala, T., Rinne, J., Räsänen, M., Leitner, S., and Pellikka, P.: Soil greenhouse gas emissions under different land-use types in savanna ecosystems of Kenya, Biogeosciences, 17, 2149–2167, https://doi.org/10.5194/bg-17-2149-2020, 2020.

Wanderley, R. L., Dominigues, L. M., Joly, C. A., and da Rocha, H. R.: Relationship between land surface temperature and fraction of anthropized area in the Atlantic forest region, Brazil, PLoS One, 14, http://dx.doi.org/10.1371/journal.pone.0225443, 2019.

https://doi.org/10.5194/bg-2021-261
Preprint. Discussion started: 21 October 2021

Biogeosciences Discussions
Open Access

Wang, L., Lu, Y., and Yao, Y.: Comparison of Three Algorithms for the Retrieval of Land Surface Temperature from Landsat 8 Images, Sensors, 19, 5049, http://dx.doi.org.libproxy.helsinki.fi/10.3390/s19225049, 2019.

Wild, J., Kopecký, M., Maeck, M., Sanda, M., Jankovec, J., and Haase, T.: Climate at ecologically relevant scales: A new temperature and soil moisture logger for long-term microclimate measurement, Agr. Forest Meteorol., 268, 40–47, https://doi.org/10.1016/j.agrformet.2018.12.018, 2019.

Zellweger, F., De Frenne, P., Lenoir, J., Rocchini, D., and Coomes, D.: Advances in Microclimate Ecology Arising from Remote Sensing, Trends Ecol. Evol., 34, 327–341, https://doi.org/10.1016/j.tree.2018.12.012, 2019.

Zellweger, F., De Frenne, P., Lenoir, J., Vangansbeke, P., Verheyen, K., Bernhardt-Römermann, M., . . . Coomes, D.: Forest microclimate dynamics drive plant responses to warming, Science, 368, 772–775, https://doi.org/10.1126/science.aba6880, 2020.

Zomer, R. J., Trabucco, A., Coe, R., Place, F., van Noordwijk, M., and Xu, J. C.: Trees on farms: an update and reanalysis of agroforestry's global extent and socio-ecological characteristics. Working Paper 179, World Agroforestry Centre (ICRAF) Southeast Asia Regional Program, Bogor, Indonesia, 2014.

Additional references in Appendix A:

Nobis, M., and Hunziker, U.: Automatic thresholding for hemispherical canopy-photographs based on edge detection, Agr. Forest Meteorol., 128, 243–250, https://doi.org/10.1016/j.agrformet.2004.10.002, 2005.

Paletto, A., and Tosi, V.: Forest canopy cover and canopy closure: comparison of assessment techniques, Eur. J. Forest Res., 128, 265–272, https://dx.doi.org/10.1007/s10342-009-0262-x, 2009.

Pellikka, P., Seed, E. D., and King, D. J.: Modelling Deciduous Forest Ice Storm Damage Using Aerial CIR Imagery and Hemispheric Photography, Can. J. Remote Sens., 26, 394–405, https://doi.org/10.1080/07038992.2000.10855271, 2000.

Ridler, T. W., and Calvard, S.: Picture Thresholding Using an Iterative Selection Method, IEEE T. Syst. Man Cyb., 8, 630–632., 1978.

Schleppi, P., Conedera, M., Sedivy, I., and Thimonier, A.: Correcting non-linearity and slope effects in the estimation of the leaf area index of forests from hemispherical photographs, Agr. Forest Meteorol., 144, 236–242, https://doi.org/10.1016/j.agrformet.2007.02.004, 2007.

Thimonier, A., Sedivy, I., and Schleppi, P.: Estimating leaf area index in different types of mature forest stands in Switzerland: a comparison of methods, Eur. J. Forest Res., 129, 543562, https://doi.org/10.1007/s10342-009-0353-8, 2010.